Electronic Supplementary Material (ESI) for RSC Advances

Supporting Information Available for:

Insight in the dynamic ligand exchange process involved in bipyridyl linked arene ruthenium metalla-rectangles

Amine Garci,[a] Simon Marti,[b] Stefan Schürch,[b] Bruno Therrien[a]*

[a]Institute of Chemistry, University of Neuchatel, Avenue de Bellevaux 51, CH-2000 Neuchatel, Switzerland

[b]Department of Chemistry and Biochemistry, University of Berne, Freiestrasse 3, CH-3012 Berne, Switzerland

*Corresponding author. E-mail: bruno.therrien@unine.ch FAX +41-32-7182511

Electronic Supplementary Material (ESI) for RSC Advances

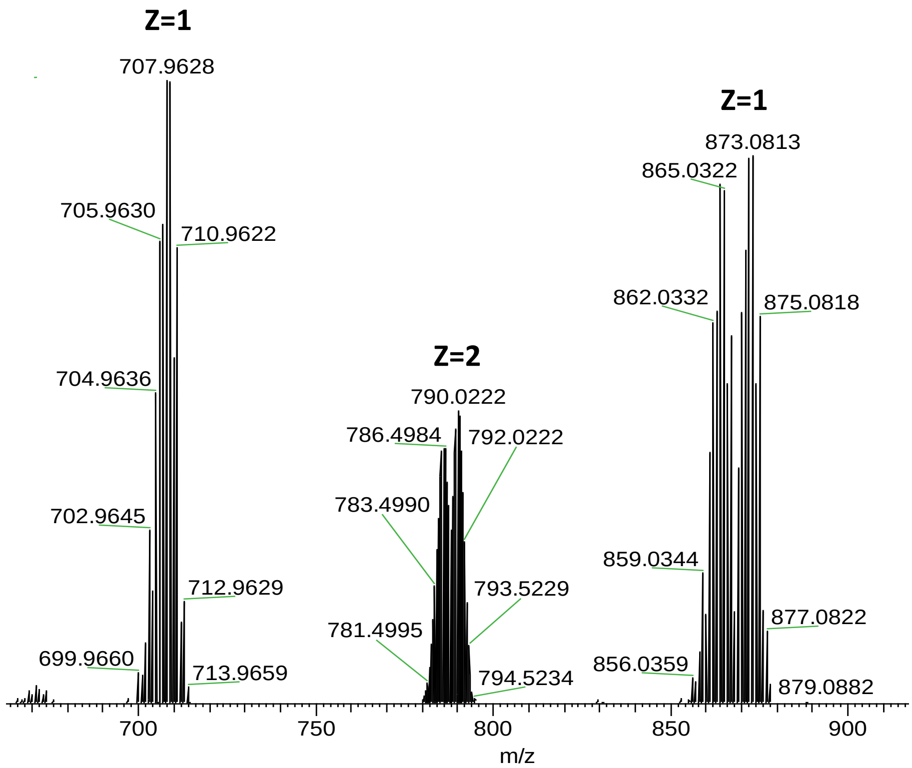

Figure S1. ESI-MS spectrum of [(p-cymene)$_4$Ru$_4$(oxalato)$_2$(bpy)$_2$](CF$_3$SO$_3$)$_4$ after mixing the two homo-rectangles (t = 0h).

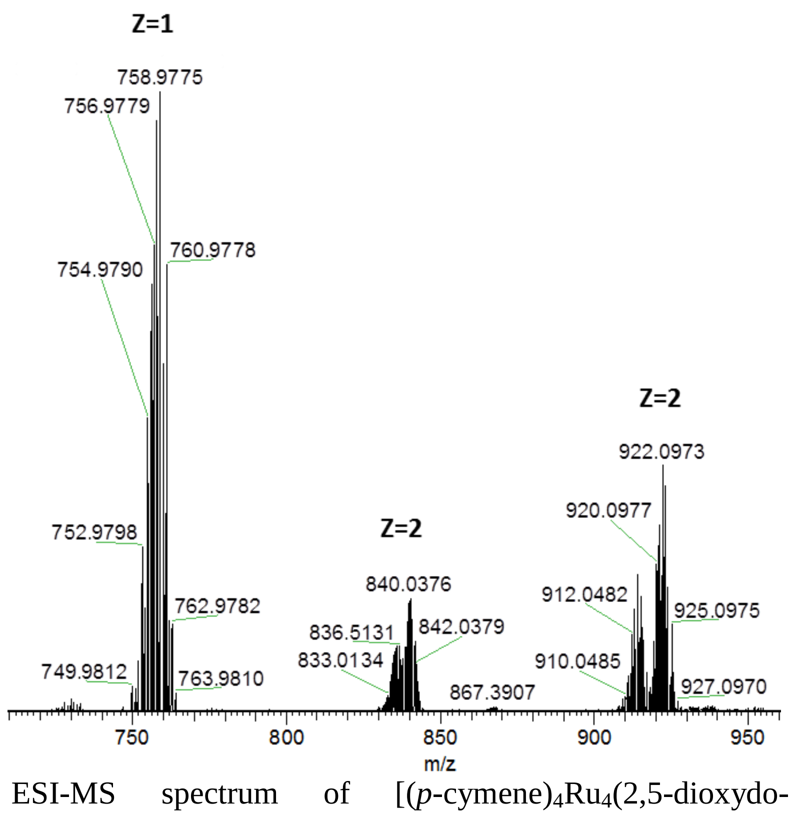

Figure S2. ESI-MS spectrum of [(p-cymene)$_4$Ru$_4$(2,5-dioxydo-1,4-benzoquino-nato)$_2$(bpy)$_2$](CF$_3$SO$_3$)$_4$ after mixing the two homo-rectangles (t = 0h).

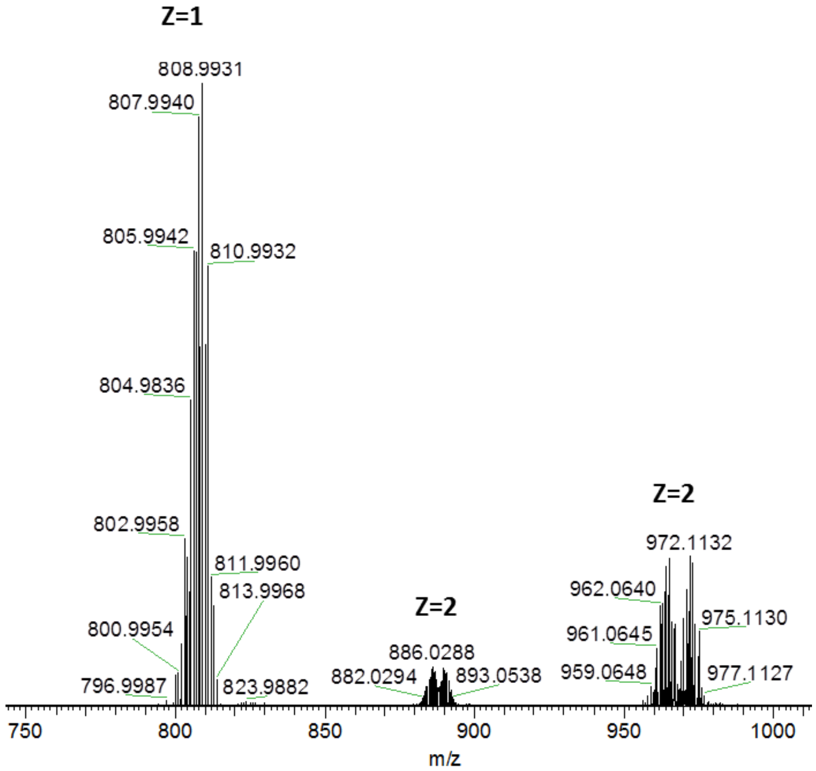

Figure S3. ESI-MS spectrum of [(*p*-cymene)$_4$Ru$_4$(5,8-dioxydo-1,4-naphtho-quinonato)$_2$(bpy)$_2$](CF$_3$SO$_3$)$_4$ after mixing the two homo-rectangles (t = 0h).

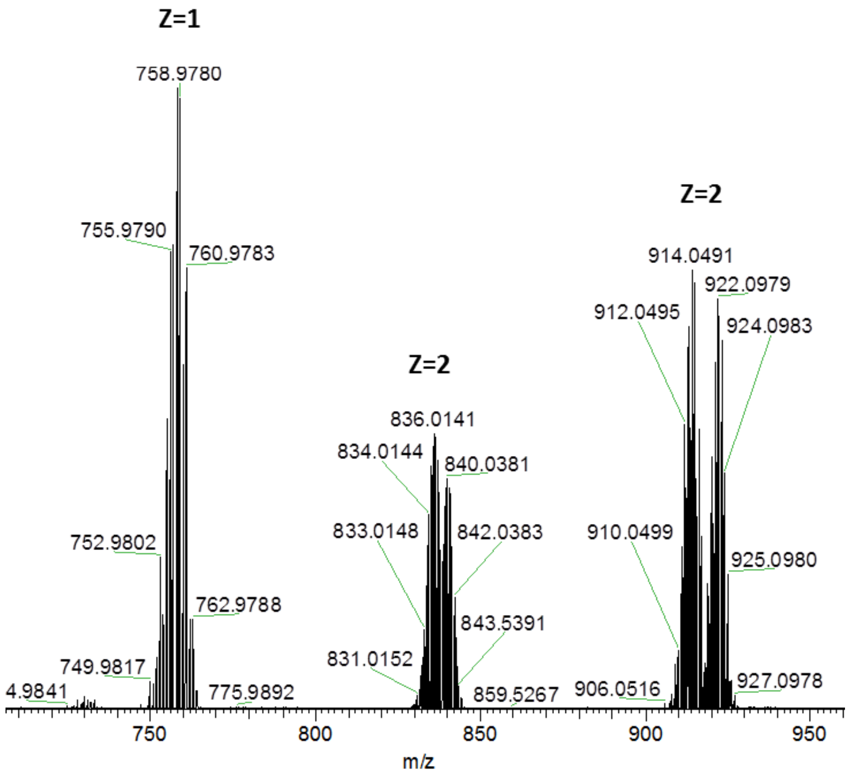

Figure S4. ESI-MS spectrum of [(*p*-cymene)$_4$Ru$_4$(2,5-dioxydo-1,4-benzoquino-nato)$_2$(bpy)$_2$](CF$_3$SO$_3$)$_4$ after mixing the two homo-rectangles (t = 14 days, 40°C).

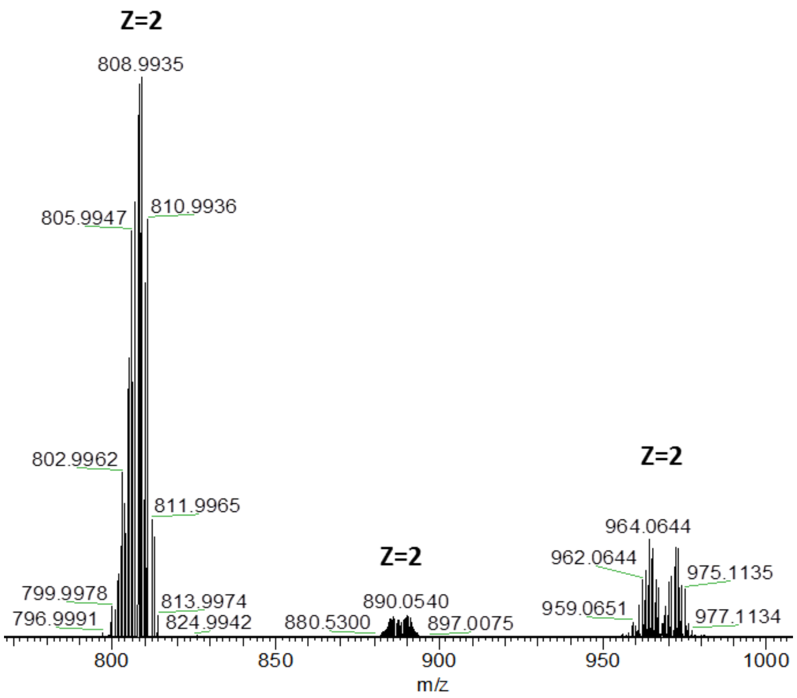

Figure S5. ESI-MS spectrum of [(*p*-cymene)$_4$Ru$_4$(5,8-dioxydo-1,4-naphtho-quinonato)$_2$(bpy)$_2$](CF$_3$SO$_3$)$_4$ after mixing the two homo-rectangles (t = 14 days, 40°C).

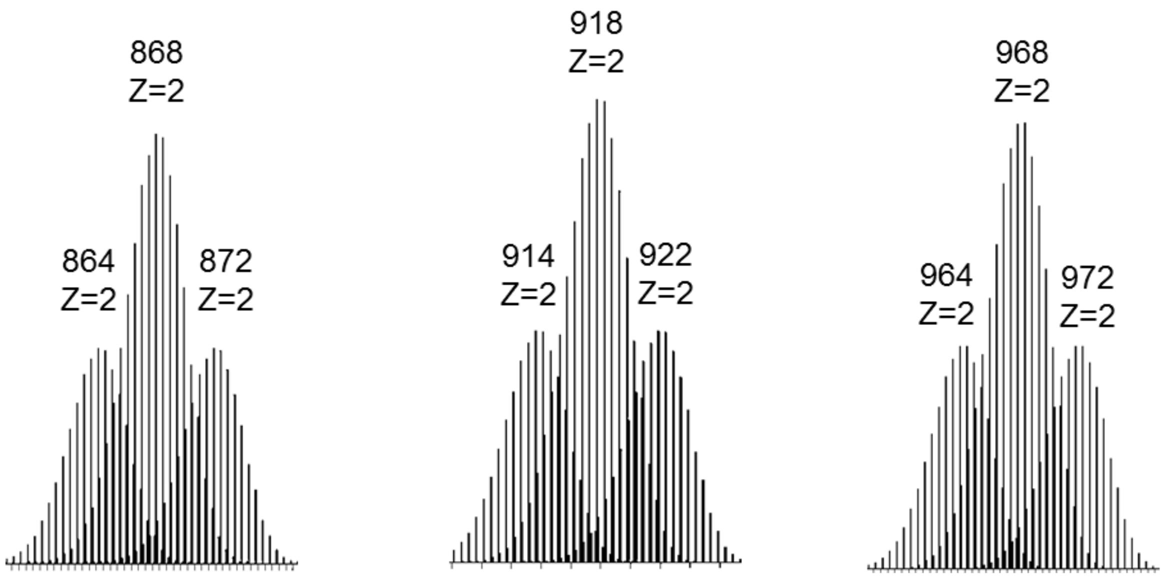

Figure S6. Calculated ESI-MS peaks corresponding to the species (in a 1:2:1 ratio), [(*p*-cymene)$_4$Ru$_4$(oxalato)$_2$(bpy)$_2$ + 2 CF$_3$SO$_3$]$^{2+}$ (left), [(*p*-cymene)$_4$Ru$_4$(2,5-dioxydo-1,4-benzoquinonato)$_2$(bpy)$_2$ + 2 CF$_3$SO$_3$]$^{2+}$ (middle) and [(*p*-cymene)$_4$Ru$_4$(5,8-dioxydo-1,4-naphthoquinonato)$_2$(bpy)$_2$ + 2 CF$_3$SO$_3$]$^{2+}$ (right).

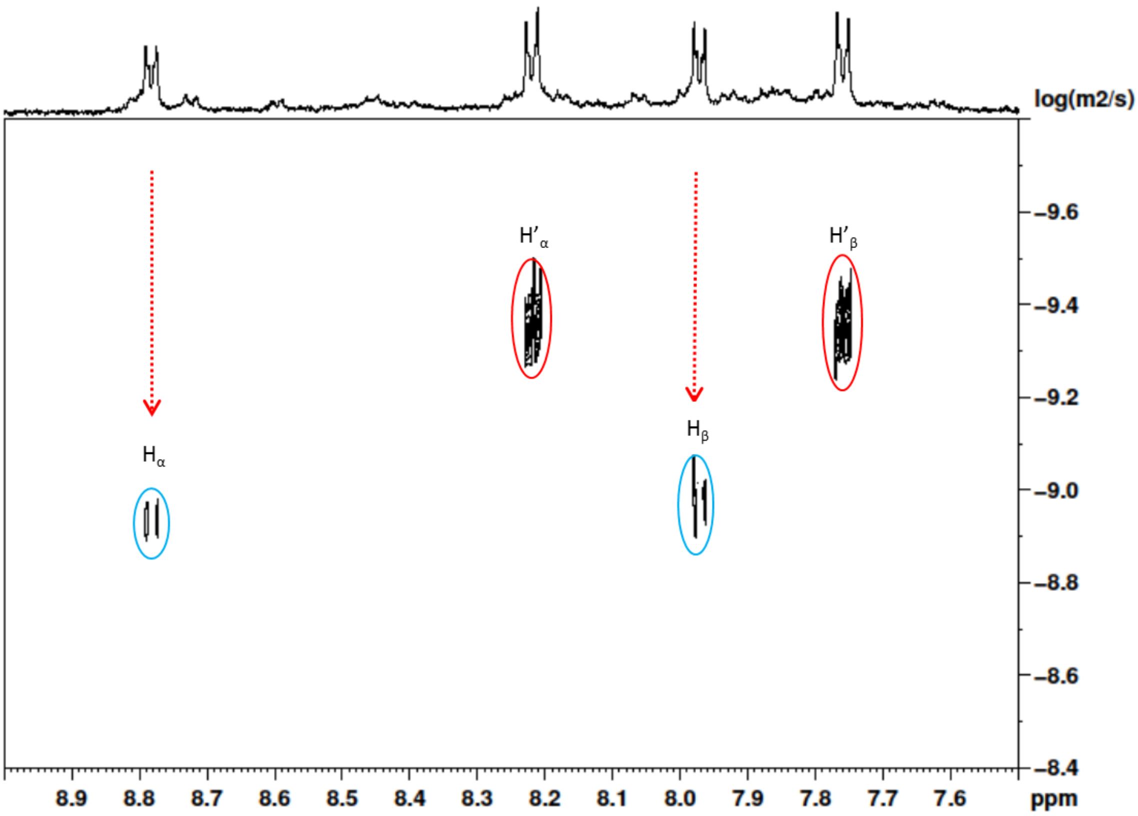

Figure S7. ^{1}H NMR and DOSY spectra (methanol-d_4, 23°C) after addition of of bpy-H_8 to [(p-cymene)$_4$Ru$_4$(oxalato)$_2$(bpy-D_8)$_2$]$^{4+}$ showing the resonances of the free bpy-H_8 (highlighted with red ovals) and the protons of the coordinated bpy-H_8 (blue ovals).

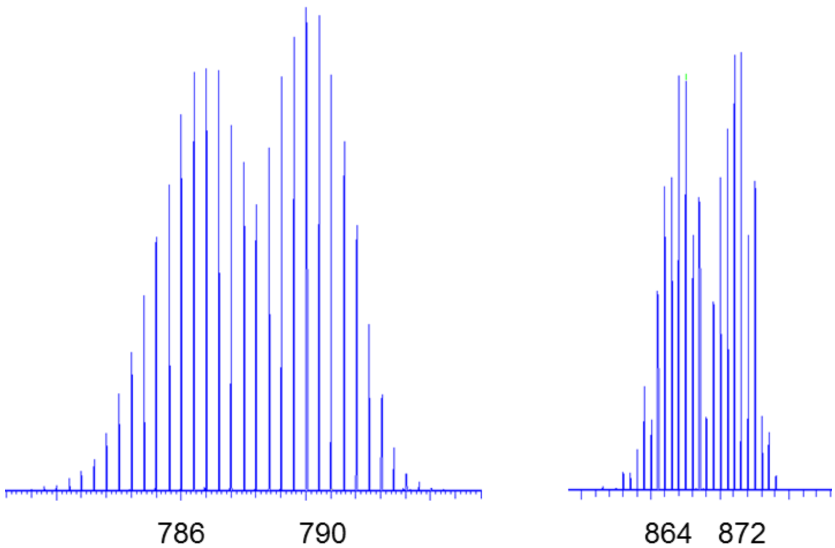

Figure S8. ESI-MS peaks corresponding to the species [(p-cymene)$_4$Ru$_4$(oxalato)$_2$(bpy) + 2 CF_3SO_3]$^{2+}$ and [(p-cymene)$_2$Ru$_2$(oxalato)(bpy) + CF_3SO_3]$^+$ (right).

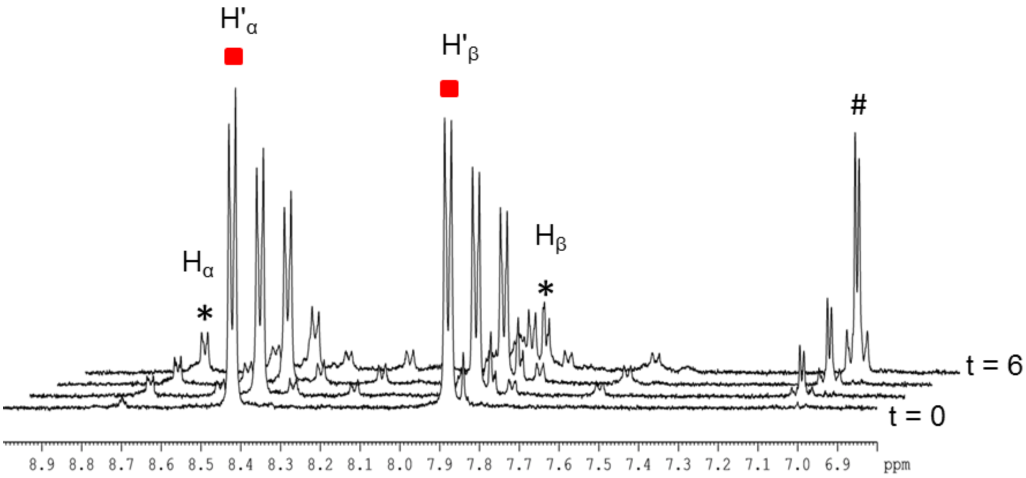

Figure S9. Representative ^{1}H NMR spectra (6 hours) following the kinetic exchange between $[(p\text{-cymene})_4Ru_4(2,5\text{-dioxydo-1,4-benzoquinonato})_2(bpy\text{-}H_8)_2]^{4+}$ (■) and bpy-D_8 (*) (methanol-d_4, 40°C), # indicates signal attributed to free *p*-cymene.

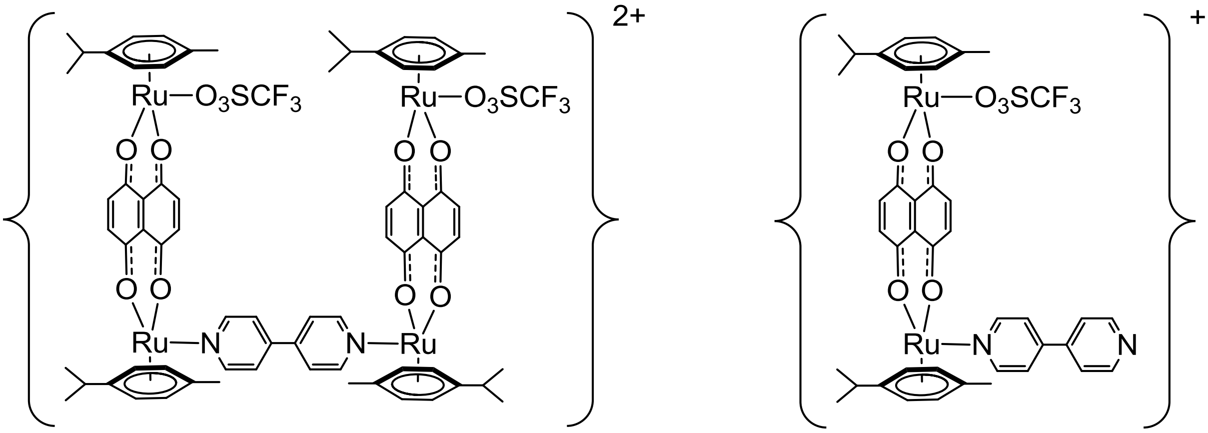

Figure S10. Molecular structure of the two fragments $[(p\text{-cymene})_4Ru_4(5,8\text{-dioxydo-1,4-naphthoquinonato})_2(bpy) + 2\ CF_3SO_3]^{2+}$ and $[(p\text{-cymene})_2Ru_2(5,8\text{-dioxydo-1,4-naphthoquinonato})(bpy) + CF_3SO_3]^{+}$.

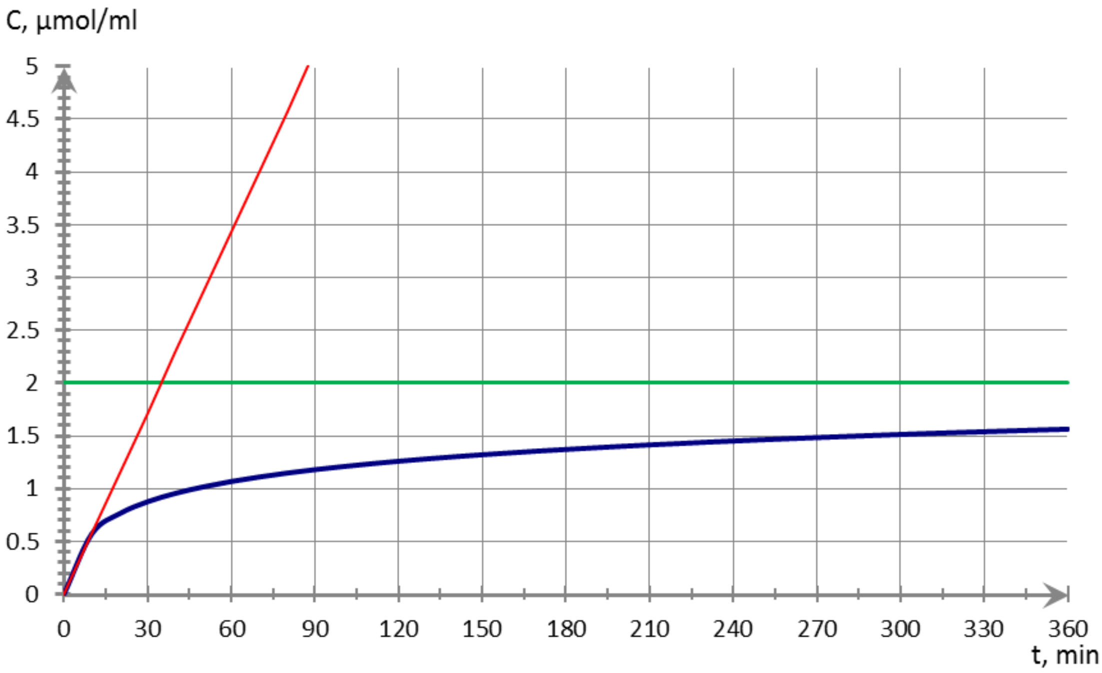

Figure S11. Initial rate of the exchange process between $[(p\text{-cymene})_4Ru_4(\text{oxalato})_2(\text{bpy-}H_8)_2]^{4+}$ and bpy-D_8 at room temperature with a 1:1 ratio.

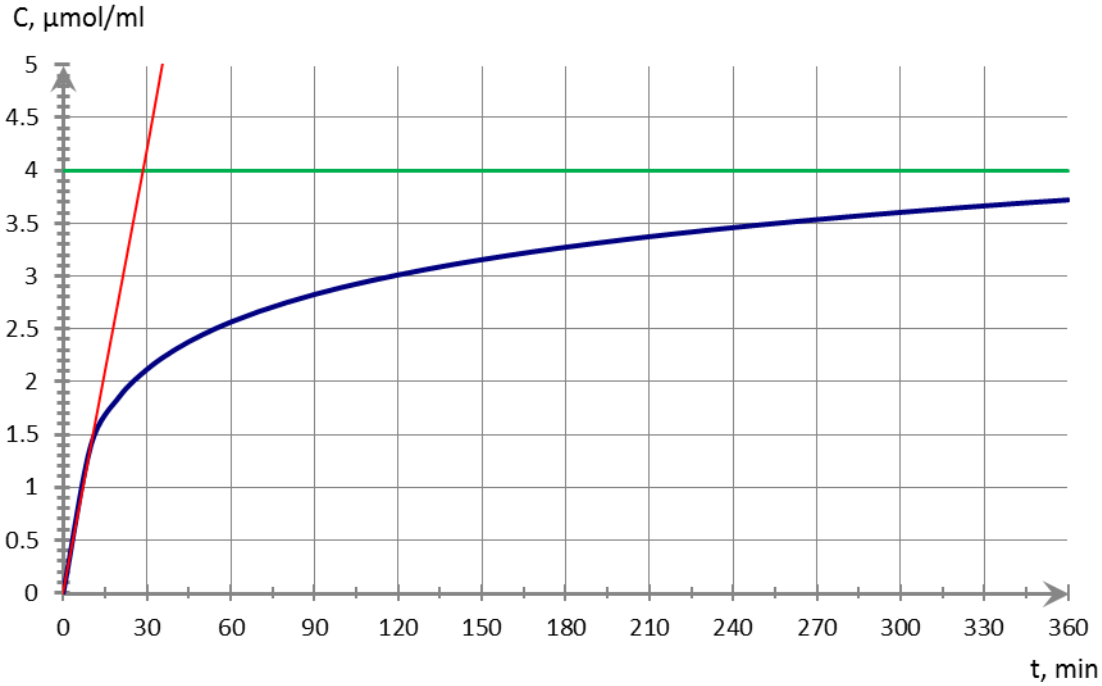

Figure S12. Initial rate of the exchange process between $[(p\text{-cymene})_4Ru_4(\text{oxalato})_2(\text{bpy-}H_8)_2]^{4+}$ and bpy-D_8 at room temperature with a 1:10 ratio.

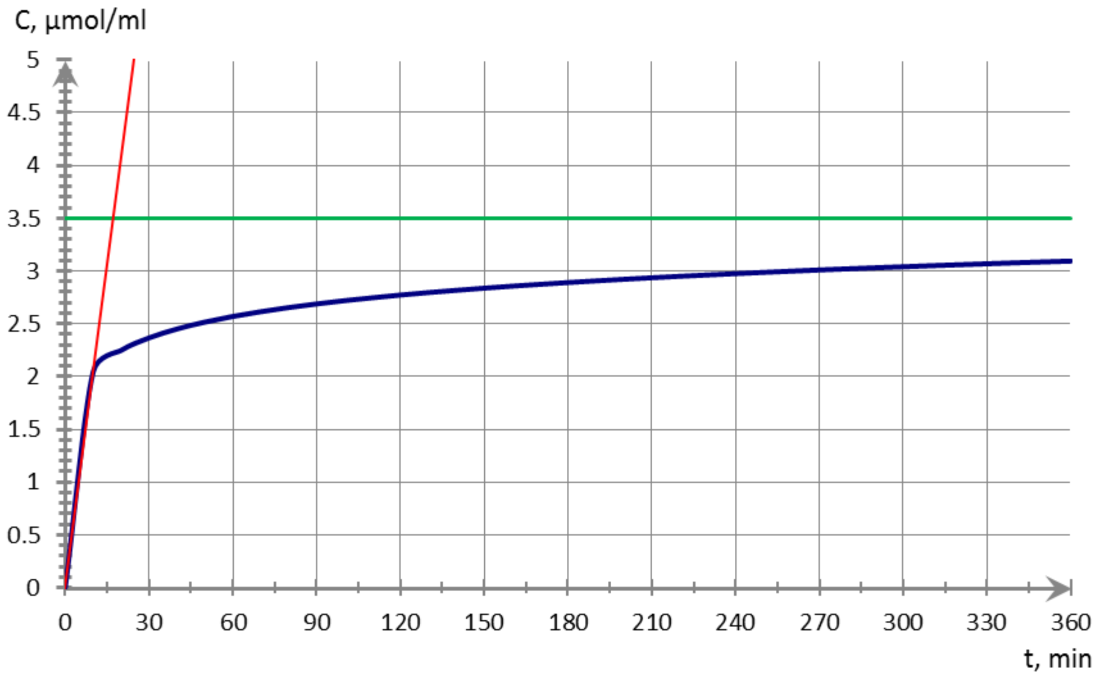

Figure S13. Initial rate of the exchange process between [(p-cymene)$_4$Ru$_4$(oxalato)$_2$(bpy-H_8)$_2$]$^{4+}$ and bpy-D_8 at 40°C with a 1:1 ratio.

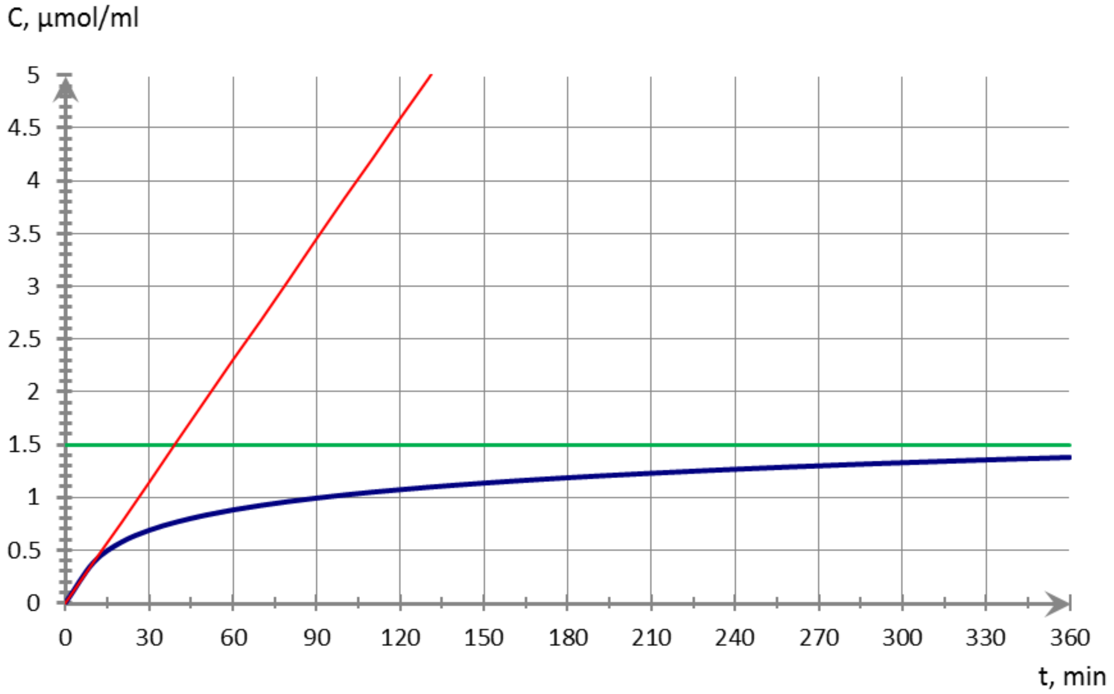

Figure S14. Initial rate of the exchange process between [(p-cymene)$_4$Ru$_4$(oxalato)$_2$(bpy-D_8)$_2$]$^{4+}$ and bpy-H_8 at room temperature with a 1:1 ratio.

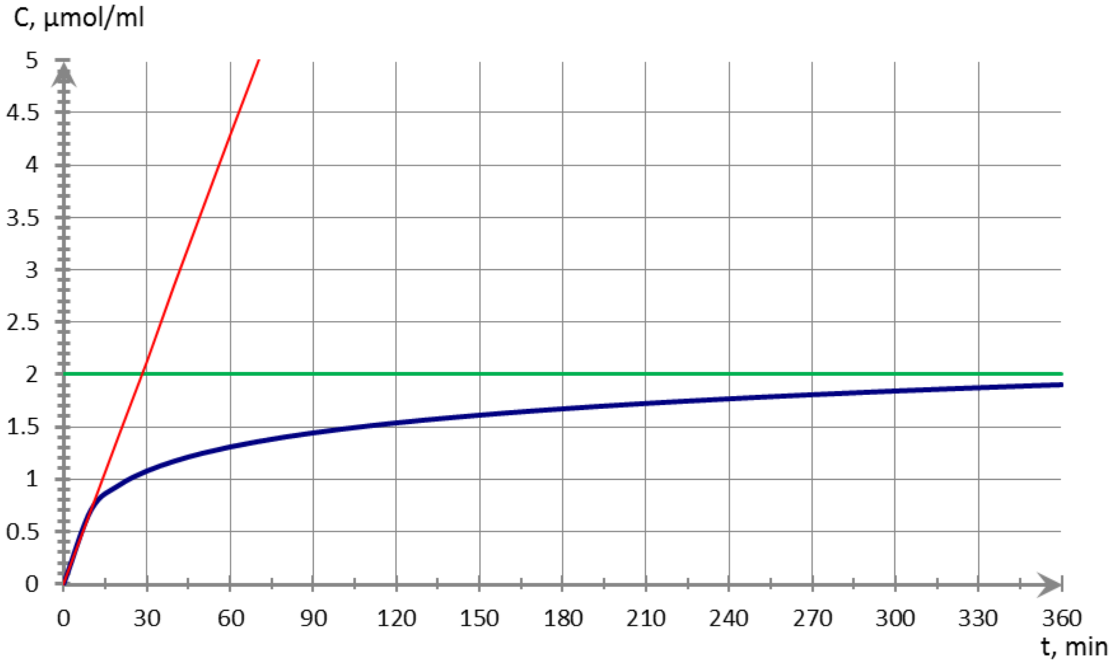

Figure S15. Initial rate of the exchange process between [(*p*-cymene)$_4$Ru$_4$(oxalato)$_2$(bpy-*D*$_8$)$_2$]$^{4+}$ and bpy-*H*$_8$ at room temperature with a 1:10 ratio.

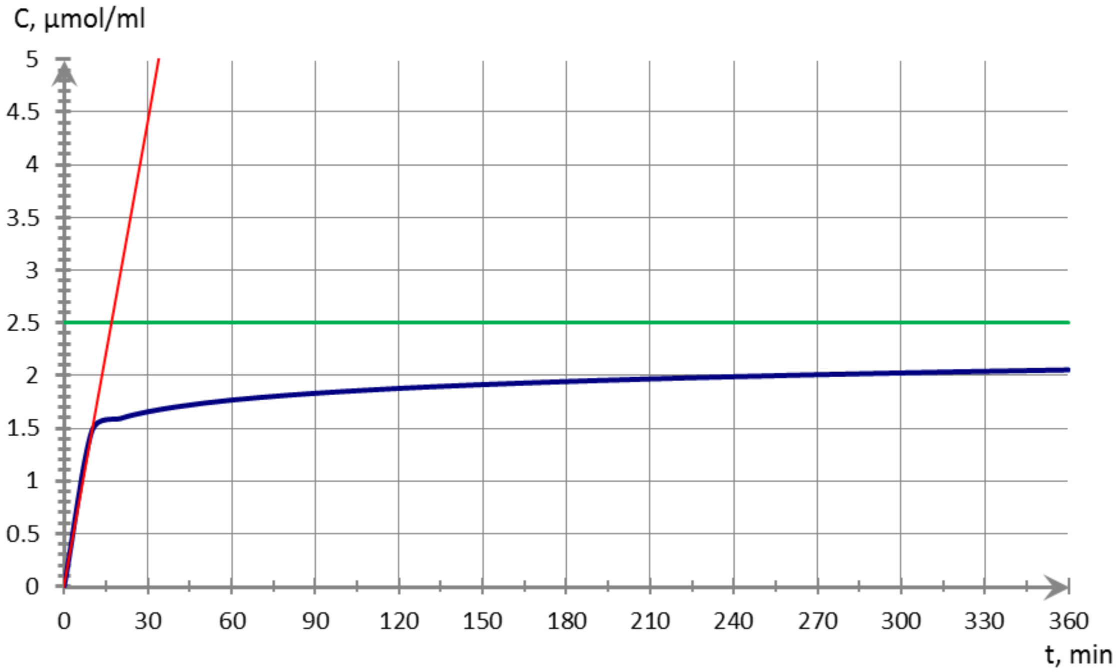

Figure S16. Initial rate of the exchange process between [(*p*-cymene)$_4$Ru$_4$(oxalato)$_2$(bpy-*D*$_8$)$_2$]$^{4+}$ and bpy-*H*$_8$ at 40°C with a 1:1 ratio.

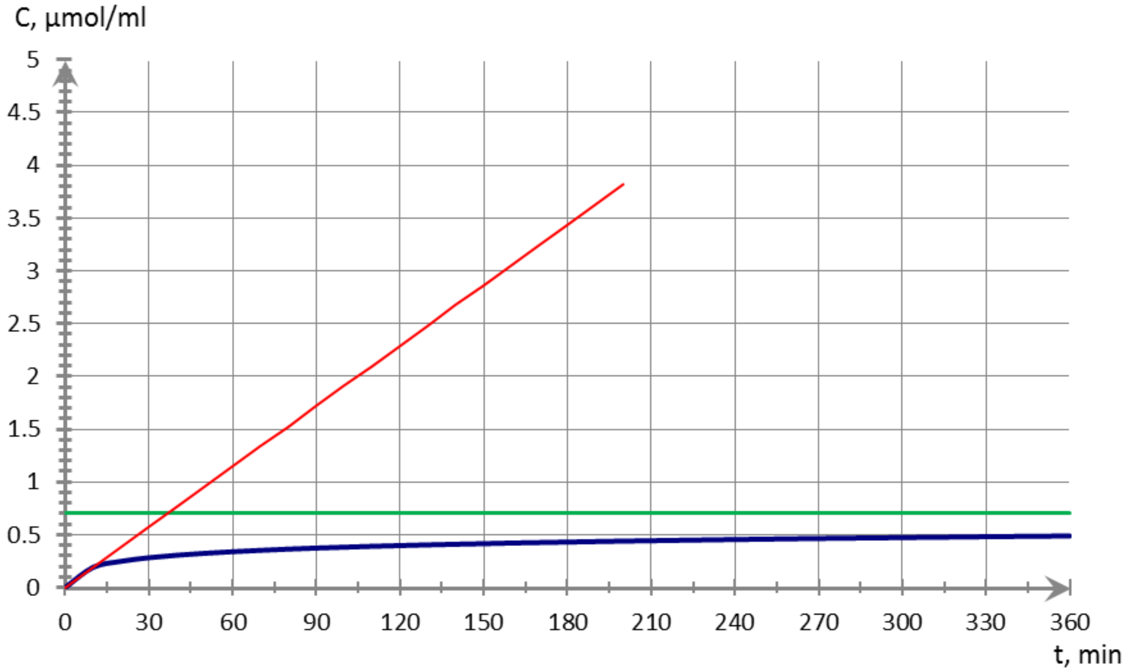

Figure S17. Initial rate of the exchange process between [(*p*-cymene)$_4$Ru$_4$(2,5-dioxydo-1,4-benzoquinonato)$_2$(bpy-H_8)$_2$]$^{4+}$ and bpy-D_8 at 40°C with a 1:1 ratio.

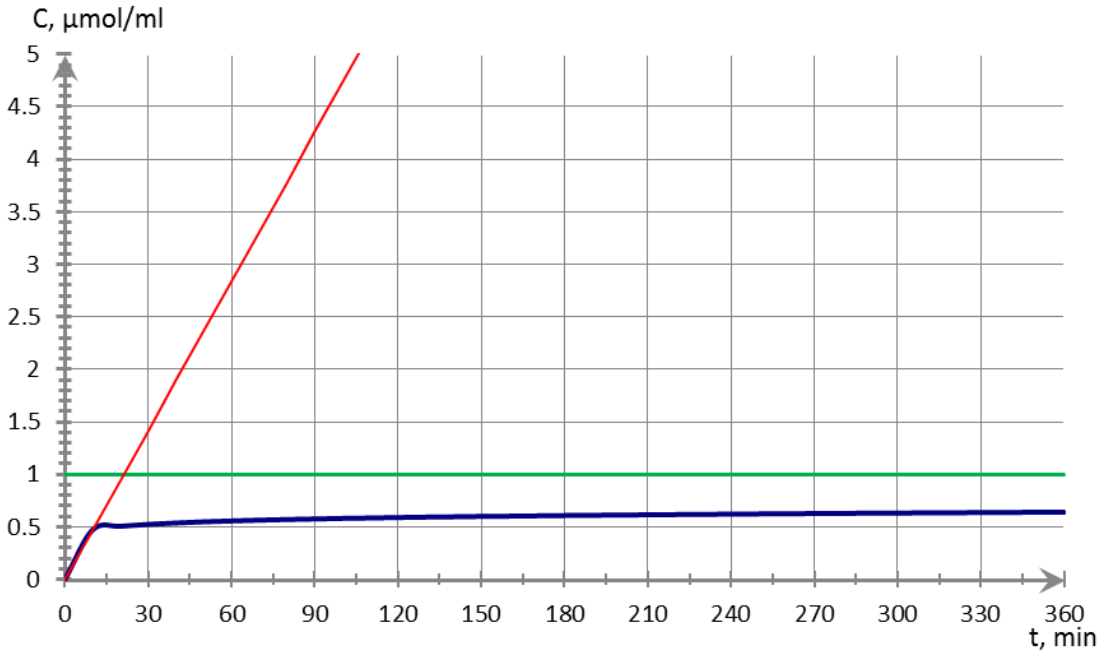

Figure S18. Initial rate of the exchange process between [(*p*-cymene)$_4$Ru$_4$(5,8-dioxydo-1,4-naphthoquinonato)$_2$(bpy-H_8)$_2$]$^{4+}$ and bpy-D_8 at room temperature with a 1:1 ratio.

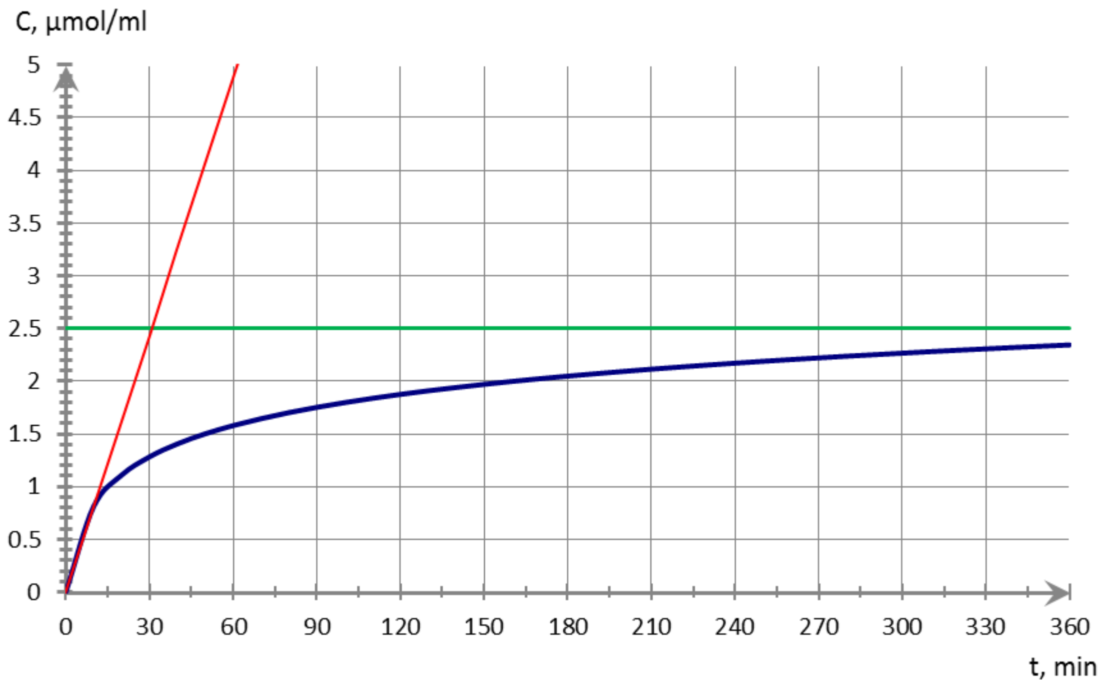

Figure S19. Initial rate of the exchange process between [(*p*-cymene)$_4$Ru$_4$(5,8-dioxydo-1,4-naphthoquinonato)$_2$(bpy-H_8)$_2$]$^{4+}$ and bpy-D_8 at room temperature with a 1:10 ratio.

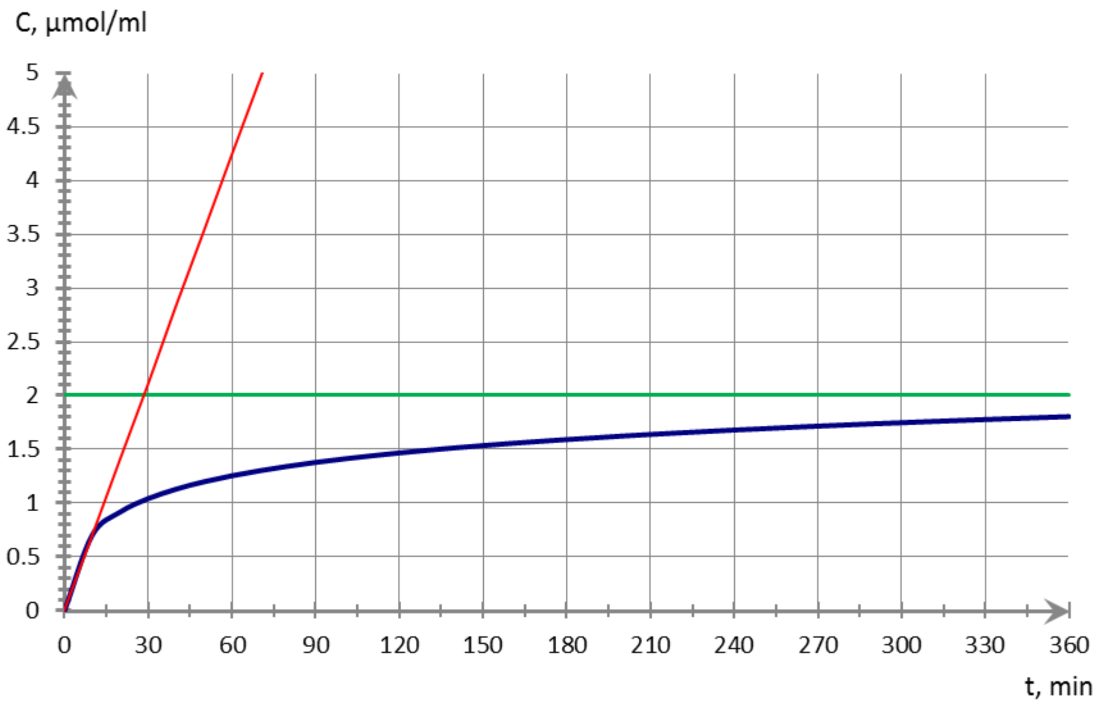

Figure S20. Initial rate of the exchange process between [(*p*-cymene)$_4$Ru$_4$(5,8-dioxydo-1,4-naphthoquinonato)$_2$(bpy-H_8)$_2$]$^{4+}$ and bpy-D_8 at 40°C with a 1:1 ratio.

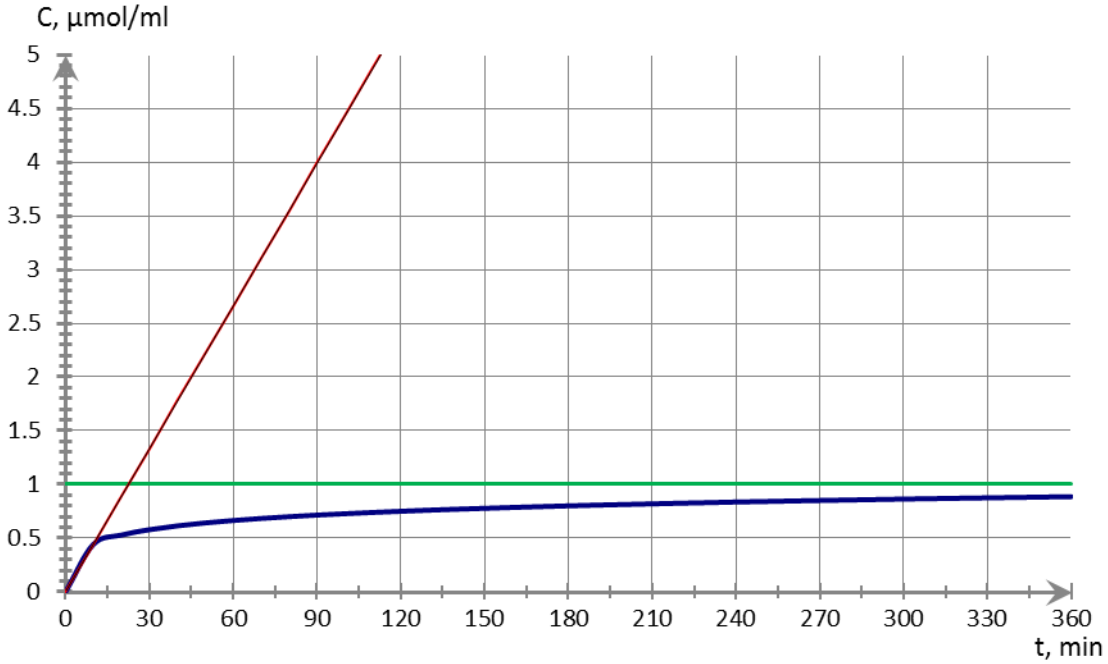

Figure S21. Initial rate of the exchange process between [(*p*-cymene)$_4$Ru$_4$(5,8-dioxydo-1,4-naphthoquinonato)$_2$(bpy-D_8)$_2$]$^{4+}$ and bpy-H_8 at room temperature with a 1:1 ratio.

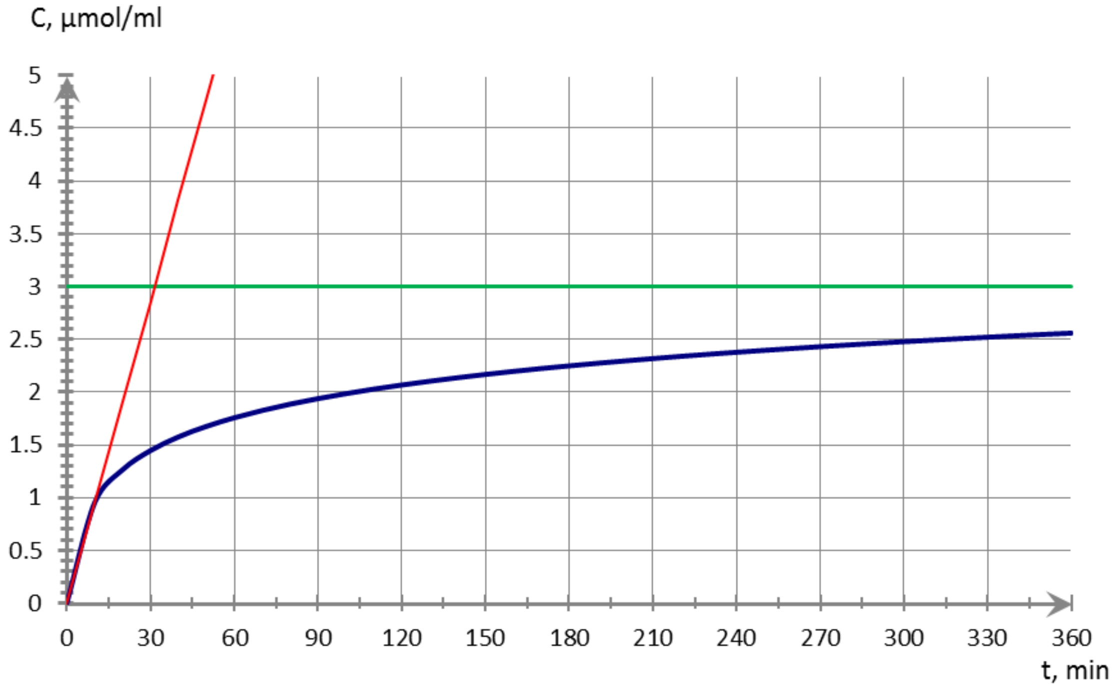

Figure S22. Initial rate of the exchange process between [(*p*-cymene)$_4$Ru$_4$(5,8-dioxydo-1,4-naphthoquinonato)$_2$(bpy-D_8)$_2$]$^{4+}$ and bpy-H_8 at room temperature with a 1:10 ratio.

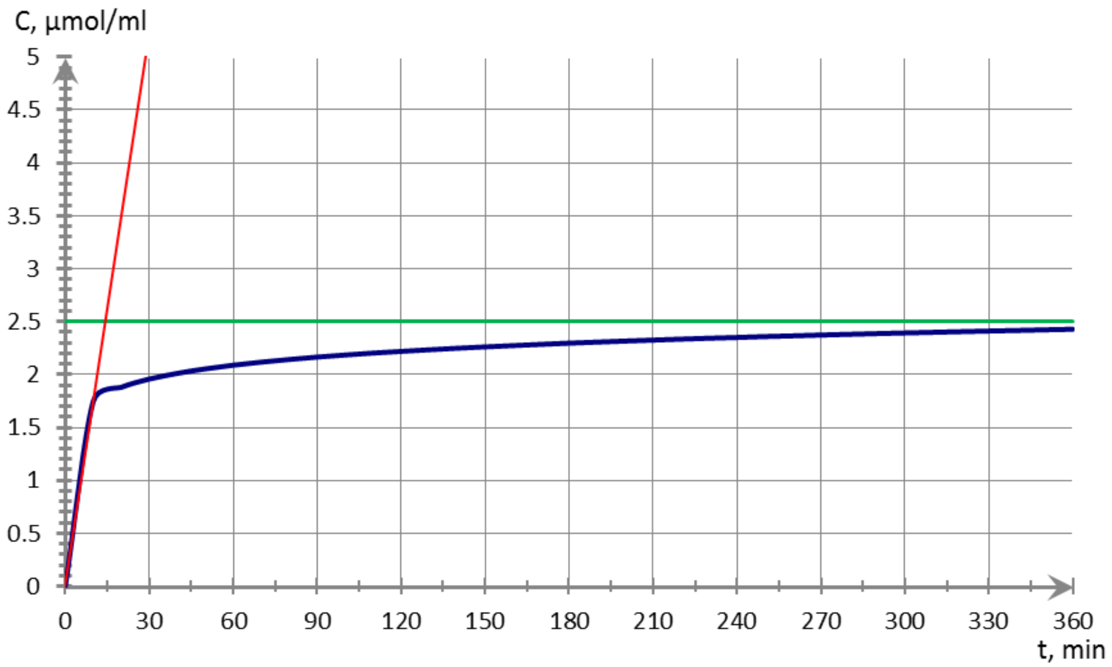

Figure S23. Initial rate of the exchange process between [(*p*-cymene)$_4$Ru$_4$(5,8-dioxydo-1,4-naphthoquinonato)$_2$(bpy-D_8)$_2$]$^{4+}$ and bpy-H_8 at 40°C with a 1:1 ratio.